Antitumor activity of pyridoisoquinoline derivatives F91873 and F91874, novel multikinase inhibitors with activity against the anaplastic lymphoma kinase

Anna Kruczynski[a], Patrice Mayer[a], Arnaud Marchand[a], Stéphane Vispé[a], Emmanuel Fournier[a], Jean-Philippe Annereau[a], Viviane Brel[a], Jean-Marc Barret[a], Georges Delsol[b], Thierry Imbert[c], Jacques Fahy[a] and Christian Bailly[a]

The anaplastic lymphoma kinase (ALK) is a validated target for the therapy of different malignancies. Aberrant expression of constitutively active ALK chimeric proteins has been implicated in the pathogenesis of anaplastic large-cell lymphoma (ALCL) and has been detected in other cancers such as inflammatory myofibroblastic tumors, diffuse large B-cell lymphomas, certain non-small-cell lung cancers, rhabdomyosarcomas, neuroblastomas and glioblastomas. In the course of a screening program aimed at identifying kinase inhibitors with novel scaffolds, the two pyridoisoquinoline derivatives F91873 and F91874, were identified as multikinase inhibitors with activity against ALK in a biochemical screen. F91873 and F91874 also inhibited nucleophosmin–ALK and signal transducer and activator of transcription 3 phosphorylation in the ALCL cell line COST with the same potency. Both F91873 and F91874 behaved as ATP noncompetitive inhibitors and inhibited cell proliferation of the ALK(+) ALCL cell lines COST, PIO, and Karpas299 ALCL. This growth inhibition effect was associated with a G_1-phase cell cycle arrest. Furthermore, administration of F91874 to severe combined immunodeficient mice bearing COST tumor xenografts resulted in a significant antitumor efficacy at 15 mg/kg/day, illustrating the potential utility of such compounds in the treatment of ALK-related pathologies. *Anti-Cancer Drugs* **20:364–372**

Anti-Cancer Drugs 2009, **20**:364–372

Keywords: anaplastic large-cell lymphoma, anaplastic lymphoma kinase, ATP noncompetitive inhibitors, in-vivo antitumor activity, kinase inhibitors, nucleophosmin–anaplastic lymphoma kinase

[a]Centre de Recherche en Oncologie Expérimentale, Institut de Recherche Pierre Fabre, Toulouse Cedex 4, [b]INSERM, Centre de Physiopathologie de Toulouse Purpan, Toulouse and [c]Centre de Recherche Pierre Fabre, Institut de Recherche Pierre Fabre, Castres, France

Correspondence to Dr Anna Kruczynski, PhD, Centre de Recherche en Oncologie Expérimentale, Institut de Recherche Pierre Fabre, Parc Technologique du Canal, 3 rue des Satellites, B.P. 94244, 31432 Toulouse, Cedex 04, France
Tel: +33 5 34 32 14 42; fax: +33 5 34 32 14 34;
e-mail: anna.kruczynski@pierre-fabre.com

Received 5 November 2008 **Revised form accepted** 10 February 2009

Introduction

Protein kinases play crucial roles in the regulation of cellular functions, such as cell proliferation, differentiation, migration, and apoptosis. Altered function of protein kinases is responsible for tumor development and progression and it is now clear that small molecule inhibitors directed toward kinases dysregulated in tumors can be clinically useful for the treatment of specific cancers [1–3]. Now there is a general agreement that the simultaneous modulation of multiple targets is often required to alter a clinical phenotype because biological redundancies and alternative pathways can often bypass the inhibition of a single target or multiple targets along a single pathway [4].

Anaplastic large-cell lymphomas (ALCLs) are a distinct subset of non-Hodgkin lymphomas, usually of T-cell origin and characterized by the expression of the CD30 antigen [5,6]. In the late 1980s, the t(2;5)(p23;q35) translocation was described as the most frequent in ALCL [7–9] and in 1994 the product of this translocation was identified as the receptor tyrosine kinase ALK, for anaplastic lymphoma kinase fused to nucleophosmin (NPM) [10]. Subsequently, other fusion partners of *ALK* were also reported in ALCL [5]. These chromosomal translocations leading to dysregulated expression and constitutive activation of the ALK protein was shown in 60–70% of ALCLs, termed ALK(+) lymphomas [11–13]. In contrast, expression of the wild-type ALK receptor in adult human tissues is restricted to selected neural and perivascular endothelial cells in the brain [14,15]. Preclinical experimental studies have shown that the aberrant expression of constitutively active ALK is implicated as a critical causative factor in the pathogenesis of ALCL and that ALK downregulation or inhibition can markedly impair the growth of ALK-positive lymphoma cells [5,16–18]. These studies and some other studies validated ALK as a target of choice for the design of new therapeutic agents active against ALK(+) ALCL.

0959-4973 DOI: 10.1097/CAD.0b013e32832a2ed9

Fig. 1

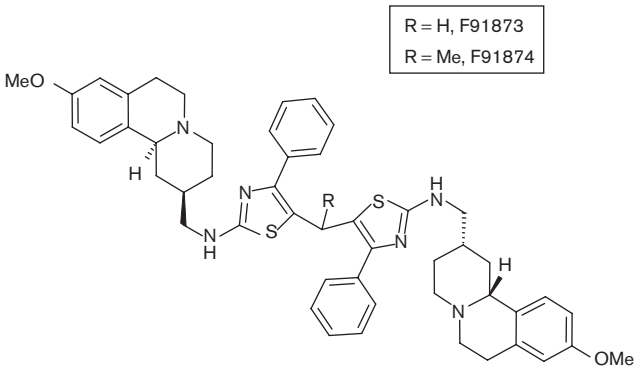

Chemical structures of F91873 and F91874. These pyridoisoquinoline derivatives are a mixture of diastereoisomers, and were not separated. H_2 and H_{11b} are in *cis* relationship as shown by ^{1}H-NMR spectra. This figure shows only one configuration.

In this study, we report the pharmacological properties of two novel multikinase inhibitors with activity against ALK: the dimeric pyridoisoquinoline derivatives F91973 and F91874, which differ by a methyl group on the central bis-thiazole unit (Fig. 1). Their effects on ALK(+) ALCL cells were investigated both *in vitro* and *in vivo* and their mechanism of action is described.

Materials and methods

Compounds

F91873 and F91874 were identified in a screening program and synthesized in Pierre Fabre Laboratories (Toulouse, France). They were solubilized in dimethyl sulfoxide (DMSO) to achieve a concentration of 1 or 0.1% in the final reaction volume for the in-vitro or cellular assays, respectively. For in-vivo studies, they were solubilized in a solution of 20% DMSO and 80% of 5% glucose.

Cells

The selected ALCL cell lines Karpas299, COST [19], and PIO ALCL cells harbor a t(2;5)(p23;q35) chromosomal translocation and express the NPM–ALK fusion protein. In contrast, FEPD cells do not express ALK and were thus selected as an ALK(–) ALCL cell line. COST, PIO, and FEPD were established by one of us (Professor G. Delsol, INSERM U563, Purpan Hospital, Toulouse, France). The other cell lines Karpas299, A549 (non-small-cell lung cancer), and SKOV3 (ovary carcinoma) were purchased from the American Type Culture Collection (Molsheim, France). COST and PIO cell lines were cultured in Iscove's modified Dulbecco's medium from 'Gibco' (Cergy, Pontoise, France) supplemented with 10% fetal calf serum, sodium pyruvate (1 mmol/l), fungizone (1.25 µg/ml) and penicillin/streptomycin (100 U/100 µg/ml). All the other cell lines were propagated in RPMI 1640 medium supplemented with 10% fetal calf serum, fungizone (1.25 µg/ml) and penicillin/streptomycin (100 U/100 µg/ml) – plus sodium pyruvate (1 mmol/l) for FEPD cells. Cell culture reagents were obtained from Gibco. Cells were maintained at 37°C in a humidified atmosphere with 5% CO_2 and maintained using standard cell culture techniques.

In-vitro kinase assays

In-vitro anaplastic lymphoma kinase activity assay

The cytoplasmic tyrosine kinase domain of ALK (according to the sequence deposited in the databank SWISS-PROT Q9UM73) was cloned into pFastBac and fused to histidine. The production was performed by GTP Technology (Toulouse, France). Enzyme activity was assayed using an enzyme-linked immunosorbent assay (ELISA)-based technique. ELISA 96-well black plates (Perkin Elmer, Coutaboeuf, France) were coated with 100 µl of GST-PLCγ1 fusion protein (Sigma, St Louis, Missouri, USA) at 0.1 mg/ml in phosphate-buffered saline (PBS) pH 7.2 (Gibco) for 3 h at room temperature. Then, wells were saturated with 200 µl of 0.5% electrophoresis grade bovine serum albumin (A7906, Sigma) in PBS pH 7.2 for 3 h at room temperature. To detect the enzymatic activity in a total volume of 100 µl per well, 0.06 µl of recombinant ALK was incubated at 30°C in the kinase reaction buffer containing, 20 mmol/l Tris–HCl pH 7.5 (Sigma), 10 mmol/l $MgCl_2$ (Sigma), 1 mmol/l DL-1-4 dithiothreitol 99% (Acros Oorganics, Geel, Belgium, USA), 60 mmol/l disodium β-glycerophosphate (TCI Europe; Zwijndrecht, Belgium) and 1 mmol/l sodium orthovanadate (Aldrich, St Louis, USA), 2% glycerol (minimum 99%, Sigma), 20 µmol/l adenosine 5′-triphosphate disodium salt (grade 1 minimum 99%, Sigma). After 45 min, wells were washed three times with 200 µl of PBS containing 0.1% Tween 20 (Sigma) and then incubated with an anti-phosphotyrosine (4G10) antibody coupled to horseradish peroxidase (Upstate, Molsheim, France) in PBS pH 7.2 containing 0.5% bovine serum albumin for 1 h at room temperature. The wells were washed again three times with 200 µl of PBS containing 0.1% Tween 20 before the signal detection with 100 µl of super signal ELISA Pico Chemiluminescent substrate (Pierce, France). Then, the luminescent signal was recorded on a Spectra Max M5 (Molecular Devices, St Grégoire, France) after a 2 min time lapse. To analyze the results, raw data were converted into percentages of inhibition according to the formula, % Inhibition = [1–(Raw Data–Negative Control)/(Positive Control–Negative Control)] × 100, where Negative Control (containing the kinase reaction buffer with 1% DMSO but without ALK) was the mean of the negative controls and Positive Control (with ALK and 1% DMSO but no compound) was the mean of the positive controls. Then a curve fitting was done on the converted data with Prism 4.03 (GraphPad Software Inc., La Jolla, California, USA). The half maximal inhibitory concentration (IC_{50}) value was calculated and corresponds to the drug concentration that inhibits 50% of ALK activity.

Other in-vitro kinase activity assays

The kinases IGF1R, PLK1, Aurora A, Aurora B, CHK1 and CAMKII were evaluated according to the same type of assay and conditions except for the following modifications: 0.05 µl IGF1R (Panvera, Madison, Wisconsin, USA) was incubated for 30 min at 30°C in 10 mmol/l imidazol pH 7.3 (Sigma), 10 mmol/l $MgCl_2$, 1 mmol/l $MnCl_2$, 10 mmol/l disodium β-glycerophosphate, 0.5 mmol/l EGTA (Sigma). PLK1 (0.5 µl) was incubated for 30 min at 30°C in ALK buffer (see above) with 1 mg/ml dephosphorylated α-casein (Sigma) as substrate. Aurora A (0.5 µl), Aurora B (1 µl), and CHK1 (1 µl) were allowed to react with 0.1 mg/ml myelin basic protein (Globozyme, Carlsbad, California, USA). CAMKII (Panvera) was incubated for 30 min at 30°C in 20 mmol/l Tris pH 7.5, 5 mmol/l $MgCl_2$, 5 mmol/l $CaCl_2$, 1 mmol/l dithiothreitol, 0.5 mmol/l EGTA, 1 µmol/l calmodulin with 0.1 mg/ml histone IIa (Sigma) as substrate. For all Ser/Thr kinases, the signal of phosphorylation was detected by an anti-phosphothreonine antibody (Cell Signaling, France) followed by a goat anti-rabbit HRP secondary antibody (Amersham, Waltham, Massachusetts, USA).

Cellular anaplastic lymphoma kinase phosphorylation assay

After seeding in 25 ml flasks, COST cells were allowed to reach logarithmic growth (48 h) before adding F91873, or F91874, or solvent (0.1% DMSO) at selected concentrations for 4 h. Then, protein lysates of COST cells were fractionated by 10% acrylamide SDS–polyacrylamide gel electrophoresis and transferred onto nitrocellulose membrane for assessment of the levels of phospho-ALK and phospho-signal transducer and activator of transcription 3 (STAT3). After blocking nonspecific sites with a Tris-buffered saline–Tween 20 solution containing 5% fat-free milk, the transfer membrane was probed overnight with an anti-phospho-Y1604-ALK (Cell Signaling) or an anti-phospho-STAT3 (Cell Signaling), followed by a 2-h incubation with a secondary antibody conjugated to peroxidase (Jackson Immuno-Research, West Grove, Pennsylvania, USA). Proteins of interest were visualized by enhanced chemoluminescence (Pierce, Rockford, Illinois, USA) and signals acquired by a CCD camera were quantified using QuantityOne software (BioRad, Ivry-sur-Seine, France). To normalize these quantifications, the same extracts were similarly processed before probing the membranes with either an anti-total ALK (Dako, Glostrup, Dennmark) or an anti-total STAT3 (Santa Cruz, California, USA).

Cell proliferation assay

The antiproliferative activity of F91873 and F91874 was measured using the ATPlite assay (Perkin Elmer). Adherent cells were seeded in 96-well plates (10^4 cells/ml for A549 and 2.5×10^4 cells/ml for SKOV3) on day 0, and then incubated for 24 h. Nonadherent cells (COST, PIO, FEPD, Karpas299) were seeded in 96-well plates (3×10^5 cells/ml) on day 1, at a concentration to ensure that cells remained in a logarithmic cell growth phase throughout the 72-h drug treatment period. All cells were treated on day 1 and then placed in a 5% CO_2 incubator at 37°C. On day 4, cell viability was evaluated by dosing the ATP released by viable cells. The IC_{50} values were determined with curve fitting analysis (nonlinear regression model with a sigmoidal dose response, variable Hill slope coefficient), performed with the algorithm provided by the GraphPad Software.

Flow cytometry analysis

After treatment of COST cells with F91873, F91874, or solvent (0.1% DMSO) as control for 24–72 h, flow cytometry was performed with the Guava EasyCyte mini system and the percentage of cells in the G_0/G_1, S, and G_2/M phase of the cell cycle were assessed using the Guava Cell Cycle reagent kit (Guava Technologies, Burlingame, California, USA). A total of 5000 ungated events were acquired for each sample. The data were further analyzed using the CytoSoft software (Guava Technologies). The number of cells represented at least 75% of all acquired events.

In-vivo studies

Mice

Female severe combined immunodeficient (SCID) mice (C.B.-17/Icr Ico-*scid*, Charles River, St Aubin-les-Elbeuf, France) were used for implanting the human COST ALCL. Animals were monitered and cared for in accordance with the Guide for the Care and Use of Laboratory Animals (National Research Council, 1996) and the European Directive EEC/86/609, under the supervision of authorized investigators.

Experimental chemotherapy

All experiments were conducted in compliance with French regulations and regional ethics committee guidelines, based on the UKCCCR guidelines for the welfare of animals in experimental neoplasia, as described earlier [20]. Subcutaneously 4×10^6 COST cells/mouse were implanted into SCID mice on day 0 and allowed to increase to a median value of 70–130 mm^3. After randomization in treatment cages, F91873 or F91874 compounds were administered intraperitoneally as daily injections over 2 weeks. Mice were checked daily, with any adverse clinical reactions noted, and deaths recorded. Mice were weighed five times weekly during treatments and twice weekly thereafter. Tumors were measured with callipers twice weekly and tumor volumes (cubic meter) were estimated as equal to 0.5 (length × width^2). Results are presented for experiments involving five mice per experimental group.

Evaluations of antitumour activity

Treatment efficacy was assessed by measuring the effects of compounds on tumor volumes of tumour-bearing relative to control vehicle-treated mice. Two evaluation

criteria were used in parallel: (i) growth inhibition, calculated as the ratio of the median tumor volumes of drug-treated (T) versus control (C) groups: T/C, % = (median tumor volume of drug-treated group on day *X*/median tumor volume of control group on day *X*) × 100, the optimal value, being the minimal T/C ratio which reflects the maximal tumor growth inhibition achieved [21]; (ii) relative area under the tumor growth curve, rAUC (%), representative of the tumor growth curve as a whole, reflects the overall effect of a test compound over time [20]. Relative AUC = median [(area under the tumor growth curve of an individual experimental mouse/median area under the tumor growth curve of the control group) × 100]. The more active the compound, the lower the rAUC value. The nonparametric Mann–Whitney Rank Sum test was used for statistical comparisons of the respective rAUC population values.

Results

Chemistry

F91873 and F91874, two closely related pyridoisoquinolines (Fig. 1) were identified as inhibitors of ALK in a biochemical enzymatic screen of an in-house chemical library of pure compounds. The synthesis of these compounds is described in the Fig. 2. Known ketone 1 [22] was reacted with TosMIC in the presence of tBuOK in DME led to the two racemic diastereoisomer nitriles 2a and 2b, which could be separated on column chromatography. Stereochemical assignments of these *cis* and *trans* nitriles, 2a and 2b, respectively, were determined by examination of their ^{1}H-NMR spectra. Reduction with AlH_3 (a mixture of $AlLiH_4$ and H_2SO_4 in THF) of *cis* nitrile 2a led to primary amine 3. Reaction of 3 with benzoylisothiocyanate in methylene chloride yielded 4, and direct saponification gave the thiourea 5. Heterocyclization of the thiourea with phenacyl bromide in ethanol smoothly furnished the phenylaminothiazole derivative 6, as starting material for dimerization. A Mannich-like reaction with formol or acetaldehyde in acidic conditions afforded F91873 and F91874, respectively. Both compounds were obtained as a mixture of their diastereoisomeric forms, they appeared as a single spot on thin layer chromatography and were not separated.

A preliminary chemical modulation of the pyridoisoquinoline structure revealed that the dimeric nature of this molecule is required for ALK inhibition as the monomers proved to be inactive. Furthermore, the modulation of the R group (Fig. 1) showed that H and CH_3 were the best substituents for ALK inhibition, followed by the phenyl group.

F91873 and F91874 are active against several protein kinases, including ALK, and inhibit cell proliferation

The activity of F91873 and F91874 was evaluated against a panel of kinases in biochemical assays, including ALK, IGF1-R, PLK1, Aurora A, Aurora B, CHK1, EGFR, PKC, DNAPK, PKA, and CAMK II. Both F91873 and F91874 inhibited ALK activity in a concentration-dependent manner, with IC_{50} values of 3 µmol/l (Table 1 and Fig. 3). F91873 and F91874 inhibited IGF1-R, Aurora B, and CHK1 as well, with IC_{50} values in the micromolar range,

Fig. 2

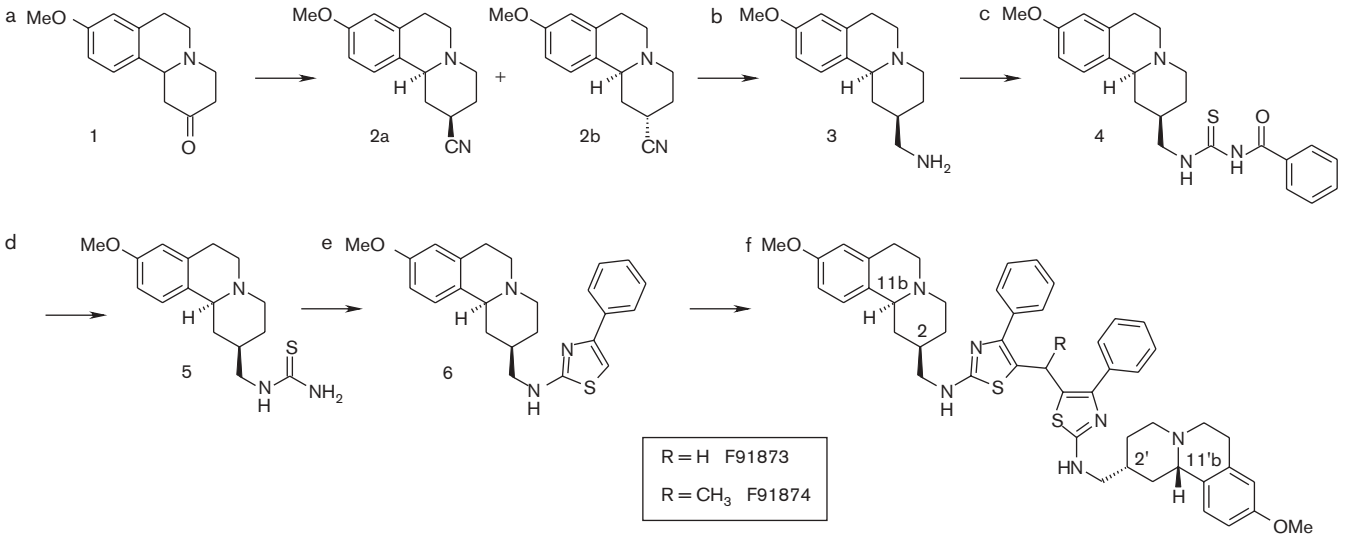

Chemical synthesis of F91873 and F91874, reagents and reaction conditions. a – TosMIC, tBuOK, DME, room temperature, 40% for 2a+2b; chromatographic separation; b – 2a, AlH_3, THF, 0°C, 86%; c – benzoylisothiocyanate, CH_2Cl_2, room temperature, 58%; d – NaOH, EtOH, reflux, 84%; e – phenacyl bromide, EtOH, room temperature, 82%; f – RCHO, formic acid, 70°C, 89%.

Table 1 F91873 and F91874 inhibit several kinases, including anaplastic lymphoma kinase

	Kinase inhibition, IC_{50}(μmol/l)						
Compound	ALK	IGF1-R	Aurora B	CHK1	Aurora A	PLK1	CAMKII
F91873	3±0.3	5±0.2	5±0.8	6±0.1	10±4	50±2	30±2
F91874	3±0.5	3±0.4	4±0.7	6±0.1	10±5	2±0.2	30±2

Kinase activity was assayed in the presence of vehicle or increasing concentrations of F91873 or F91874, using an ELISA-based technique. IC_{50} values (±standard deviations) are representative of two independent experiments.
ELISA, enzyme-linked immunosorbent assay; IC_{50}, half maximal inhibitory concentration.

Table 2 F91873 and F97874 inhibit tumor cell proliferation

	Inhibition of cell proliferation, IC_{50}(μmol/l)		
Compound	FEPD	A549	SKOV3
F91873	3.1±0.2	1.4±0.3	2.0±0.3
F91874	2.4±0.8	1.6±0.5	1.9±0.2

Designated cell lines were treated with increasing concentrations of F91873 or F91874 or vehicle for 72 h. An ATPlite assay was carried out to determine the relative cell numbers. IC_{50} values (±standard deviations) are representative of two independent experiments.
IC_{50}, half maximal inhibitory concentration.

Fig. 3

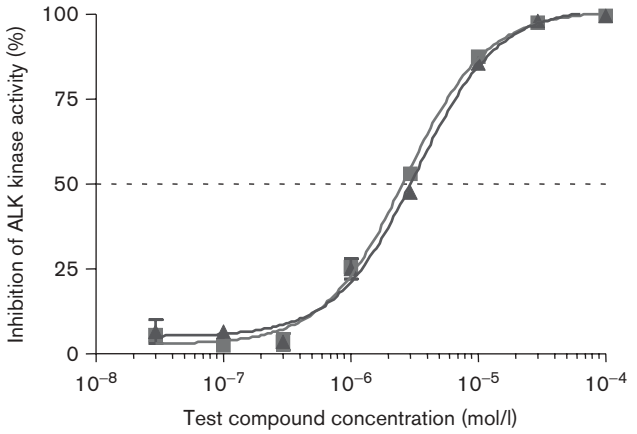

F91873 and F91874 inhibit anaplastic lymphoma kinase (ALK) activity. ALK activity was assayed in the presence of increasing concentrations of F91873 (squares) or F91874 (triangles), using an ELISA-based technique. A curve fitting was carried out with Prism 4.03 (GraphPad Software Inc.) on data, expressed as percentage of inhibition of ALK activity, as described in the Materials and methods. Data are representative of two independent experiments carried out in sextuplet.

Fig. 4

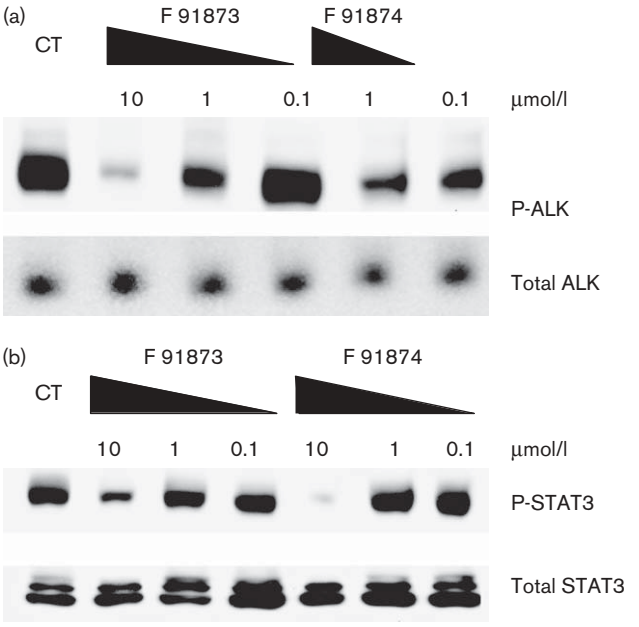

F91873 and F91874 inhibit tyrosine phosphorylation of nucleophosmin–anaplastic lymphoma kinase (ALK) and signal transducer and activator of transcription 3 (STAT3) in COST anaplastic large-cell lymphoma cells. Western blot analyses of the level of phospho-Y1604-ALK (a) or phospho-STAT3 (b) in COST cells after treatment with drug vehicle (CT: dimethyl sulfoxide 0.1%) or increasing concentrations of F91873 or F91874 for 4 h. Loading controls are represented by the quantification of total ALK and total STAT3 levels. Data are representative of two independent experiments.

that is, 3–6 μmol/l, whereas they showed an approximately 10-fold lower activity against CAMK II (Table 1). Interestingly, F91874 exhibited a more potent inhibitory activity against PLK1 than F91873, with an IC_{50} value of 2 versus 50 μmol/l. In contrast, these compounds did not induce any inhibition against EGFR, DNA-PK, PKA, and PKC (data not shown).

Furthermore, F91873 and F91874 impaired the growth of several tumor cell lines, namely FEPD (ALCL), A549 (lung) and SKOV3 (ovary), with similar values of IC_{50}, that is, 1–2.5 μmol/l (Table 2).

F91873 and F91874 inhibit anaplastic lymphoma kinase in a cell-based specificity screen

In a cell-based specificity screen, using the COST cell line as a model of ALK(+) ALCL, F91873 and F91874 inhibited tyrosine phosphorylation of NPM–ALK, also in a concentration-dependent manner, with IC_{50} values of 5 and 1 μmol/l, respectively (Fig. 4a). Furthermore, F91873 and F91874 inhibited the phosphorylation of STAT3, one of the various partners of NPM–ALK, with IC_{50} values of 8 and 2 μmol/l, respectively, in COST cells (Fig. 4b). This first set of data indicates that the two compounds inhibit the phosphorylation of both the target kinase and its substrate.

F91873 and F91874 are ATP noncompetitive inhibitors of anaplastic lymphoma kinase

To determine the mechanism of drug-induced inhibition, kinase assays with increasing ATP concentrations were performed. At high ATP concentrations, a weak but reproducible decrease in signal was observed, even in the

absence of inhibitory compound (Fig. 5a and b). This type of behavior can easily be explained by substrate inhibition. Consequently, data were fitted to a modified Michaelis–Menten equation accounting for the decrease in signal at high ATP concentration [23], as follows: $v = V_{max} \times [S]/(K_m + [S] \times (1 + [S]/K_i^S)$, where 'S' is the ATP concentration and K_i^S is the substrate inhibition constant (K_i^S approximately 17 mmol/l). For a given concentration, the capacity of F91873 and F91874 to inhibit the catalytic activity of ALK was not decreased in the presence of increasing concentrations of ATP, suggesting that these pyridoisoquinoline compounds were not displaced by the natural ligand of ALK (Fig. 5a and b). Considering the fixed GST-PLCγ1 (ALK substrate) assay concentration, apparent V_{max} and K_m obtained by nonlinear regression curve fitting (modified Michaelis–Menten equation) were used to generate Lineweaver–Burk 1/v versus 1/ATP concentration graphs. The reciprocal plots clearly highlight the noncompetitive binding behavior of both compounds regarding the ATP binding on ALK (Fig. 5c and d). This second dataset shows that F91873 and F91874 do not bind to the ATP-binding site of ALK.

F91873 and F91874 inhibited cell proliferation in a series of ALK(+) ALCL cells

As the NPM–ALK fusion protein is implicated in the dysregulation of cell growth pathways, the effects of F91873 and F91874 on cell growth in ALCL lines were evaluated. ALCL cell lines expressing a high level of NPM–ALK were chosen for this assay, namely Karpas299, COST, and PIO. Treatment of these cells with F91873 or F91874 led to a significant inhibition of cell proliferation, with IC_{50} values ranging from 1 to 5 µmol/l (Table 3).

Table 3 Effects of F91873 and F97874 on growth of ALK(+) ALCL cells

	Inhibition of cell proliferation, IC_{50}(µmol/l)		
Compound	Karpas299	COST	PIO
F91873	1.4 ± 0.3	2.0 ± 0.5	4.6 ± 1.5
F91874	1.0 ± 0.1	1.4 ± 0.3	3.5 ± 0.3

Designated cell lines were treated with increasing concentrations of F91873 or F91874 or vehicle for 72 h. An ATPlite assay was carried out to determine the relative cell numbers. IC_{50} values (± standard deviations) are representative of two independent experiments.
ALCL, anaplastic large-cell lymphoma; ALK, anaplastic lymphoma kinase; IC_{50}, half maximal inhibitory concentration.

Fig. 5

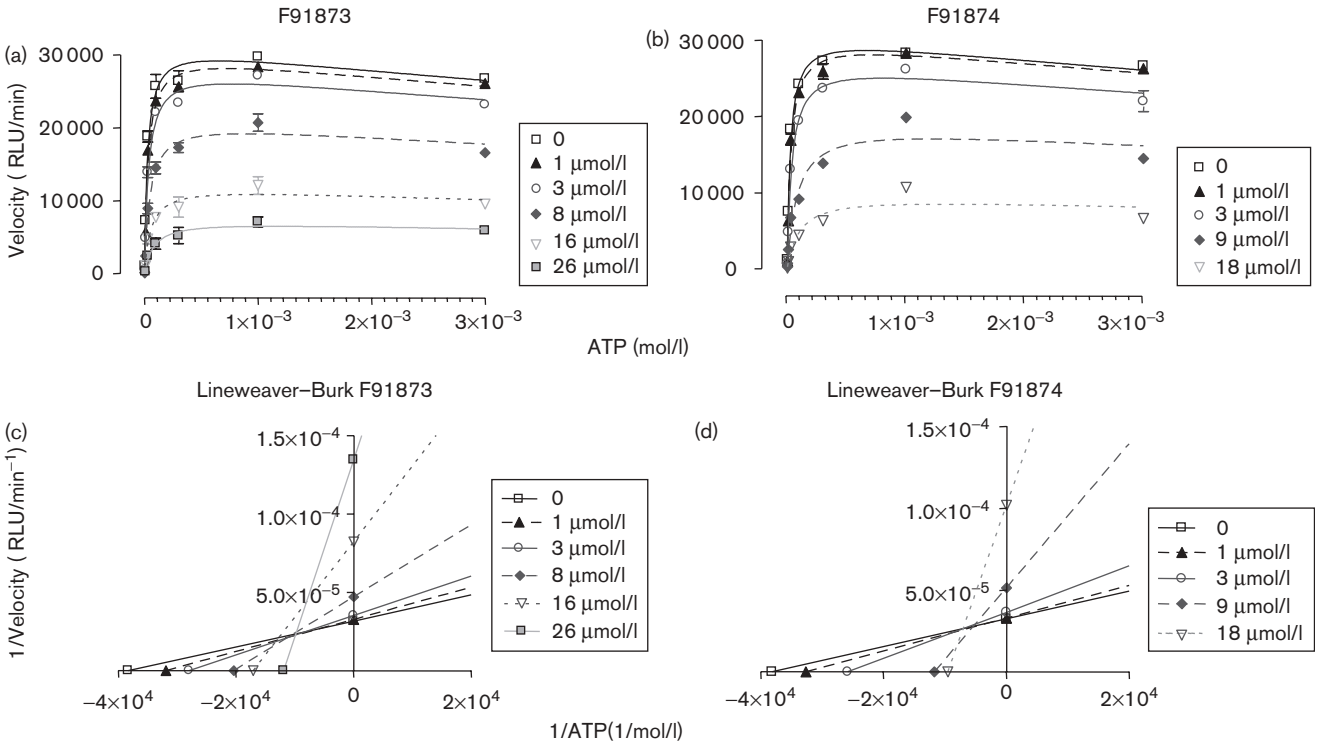

F91873 and F91874 are noncompetitive inhibitors for ATP. Anaplastic lymphoma kinase activity was assayed in the presence of increasing concentrations of ATP for each indicated concentration of inhibitor F91873 (a and c) or F91874 (b and d). (a and b) Data were fitted to a modified Michaelis–Menten equation, as follows: $v = V_{max} \times [S]/(K_m + [S] \times (1 + [S]/K_i^S)$, where '$S$' is the ATP concentration and K_i^S is the substrate inhibition constant. (c and d) Data were represented as Lineweaver–Burk double-reciprocal, 1/velocity versus 1/ATP concentration plots. Data are representative of two independent experiments.

A flow cytometric analysis of cell cycle distribution of unsynchronized COST cells was performed to further characterize the mechanism of growth inhibition (Fig. 6). As both compounds induced similar effects, only one of them, namely the methylated derivative F91874 was selected for this assay. F91874 induced a concentration-dependent increase in the number of cells in G_1 phase and a decrease in the number of cells in S and G_2 phases at 24 and 48 h (Fig. 6), respectively, which were persistent at 72 h (data not shown). At a 2.8 µmol/l concentration ($2 \times IC_{50}$) for which more than 50% of ALK phosphorylation was inhibited, F91874 induced approximately a 2-fold decrease in the number of COST cells in S phase (Fig. 6).

Fig. 6

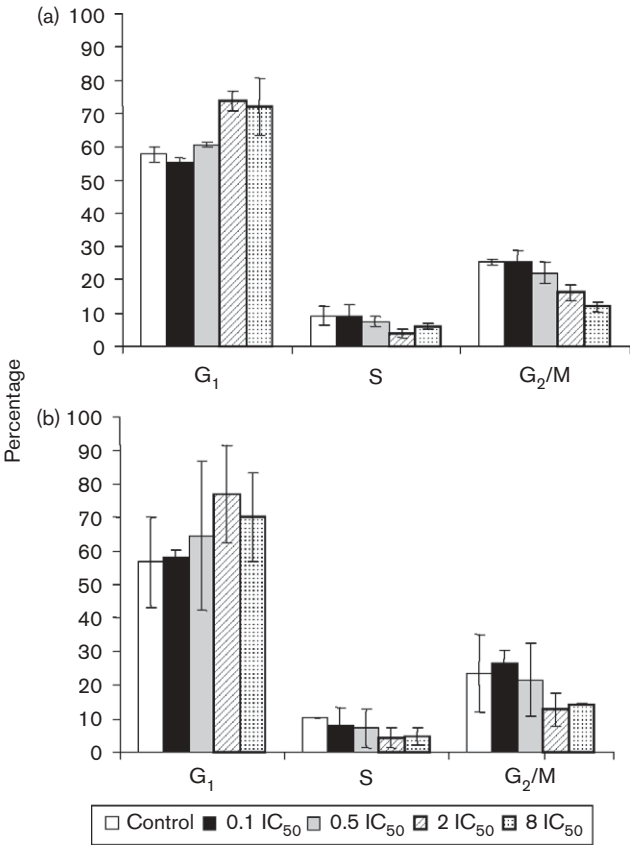

F91874-induced G_1-phase cell cycle arrest in COST anaplastic large-cell lymphoma cells. COST cells were treated with drug vehicle (dimethyl sulfoxide 0.1%) (white bars) or increasing concentrations of F91874, namely, 0.1 × half maximal inhibitory concentration (IC_{50}) (black bars), 0.5 × IC_{50} (grey bars), 2 × IC_{50} (hatched bars), or $8 \times IC_{50}$ (dotted bars) concentrations (0.14, 0.7, 2.8, and 11.2 µmol/l, respectively) for 24 h (a) or 48 h (b) in growth medium. Cell cycle distribution was assessed by fluorescence-activated cell sorting as described in Materials and methods. Data, representative of two independent experiments, are expressed as means with standard deviations. RLU, relative luminometric units.

Fig. 7

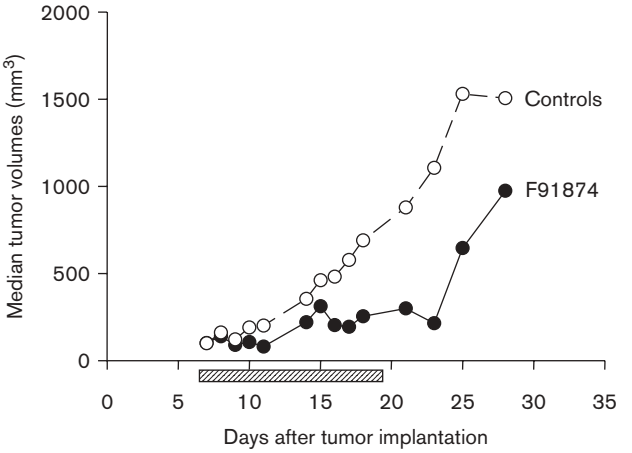

F91874 inhibits the growth of COST anaplastic large-cell lymphoma tumor xenografts. Responses of human COST xenografted tumors to 15 mg/kg per injection F91874 (●), relative to control vehicle-treated mice (○). Subcutaneously 4×10^6 cells were implanted into severe combined immunodeficient mice and, when tumors had reached a volume of 70–130 mm^3, mice were randomized and treatments were given intraperitoneally as daily administrations over 2 weeks, starting on day 7 after tumor cell implantation. The hatched bar represents the period of treatment.

F91874 inhibits tumor growth in the ALK(+) COST tumor xenograft model

COST tumors were implanted subcutaneously in SCID mice and formed established tumors that were used to evaluate the in-vivo antitumor activity of F91874. The compounds effects on the median tumor volumes of COST tumor-bearing mice relative to control animals were measured over time (Fig. 7). The administration of F91874 at 15 mg/kg/day resulted in a significant tumor growth inhibition, as reflected by an optimal T/C ratio of 19%, recorded on day 23, that is, 2 days after the end of treatment (Fig. 7). Furthermore, it is noticeable that this growth inhibition was sustained over time with significant T/C ratios, that is, $\leq 42\%$, according to the NCI criteria, of 19–42%, recorded from day 16 to 25. A significant ($P < 0.01$) rAUC measurement of 47%, indicative of an overall tumor growth inhibition of 53% was also obtained at this dose. These daily administrations of F91874 over 2 weeks at the most effective dose of 15 mg/kg/day resulted in body weight losses of less than 20% of the initial body weight. Furthermore, these body weight losses were reversible and mice fully recovered their initial body weight within 1 week after the end of treatment. At the higher dose of 20 mg/kg/day, partial tumor regressions were observed in all the five mice (data not shown). However, this dose was associated with toxicity.

Discussion

NPM–ALK and related ALK fusion proteins, commonly observed in ALCL, possess transforming potential, likely

mediated by their constitutive kinase activity. Currently, there is no optimal therapeutic regimen for ALK(+) ALCL. Doxorubicin-based combination chemotherapy has limited effectiveness, resulting in a substantial number of patients with a poor outcome, either failing to enter remission or relapsing within a few months from the start of treatment [24]. There is an obvious medical need for the treatment of these ALCL and the targeting of ALK-containing fusion protein kinases offer promising opportunities to design new effective drugs, following of Glivec-like approach.

In this study, we have identified two new pyridoisoquinoline compounds as multikinase inhibitors, with activity against ALK. The inhibitory effects of these small molecules against the recombinant enzyme have been confirmed in functional cellular assays. A satisfactory correlation can be established between the drug concentrations necessary for the inhibition of NPM–ALK phosphorylation, limitation of cell growth of ALK(+) cells, and induction of a cell cycle arrest of ALK(+) cells. This suggests that the antiproliferative effects observed in ALCL cells are, at least in part, because of inhibition of ALK and this activity translates into a significant in-vivo antitumor efficacy as observed with the COST xenograft model of ALK(+) ALCL.

Previous studies have described selective small molecule inhibitors of NPM–ALK that bind to the ATP-binding site of the enzyme, therefore inhibiting the catalytic activity of ALK by preventing the binding of ATP [17]. In contrast, the pyridoisoquinolines F91873 and F91874 are ATP noncompetitive inhibitors that do not bind to the ATP-binding site of ALK. We can hypothesize that the drugs bind to an allosteric site of ALK distinct from the ATP pocket so as to alter the conformation of the enzyme, whereby preventing the access of the enzyme substrate. Allosteric sites are important in the control of enzymes, in the case, for example, of the feedback control loop where the final product controls its own synthesis. Furthermore, the presence of highly conserved mutable residues in the enzyme ATP-binding site appears to be responsible for resistance development observed with many ATP competitive kinase inhibitors [25]. For example, Gumireddy *et al.* [25] have chosen to design compounds that do not compete for the ATP-binding site of BCR-ABL, because such compounds offer the potential to be unaffected by mutations that make chronic myelogenous leukemia cells resistant to imatinib. Several other tumor-active ATP noncompetitive kinase inhibitors have been described [26,27], such as tertiary aromatic amines targeting the IGF1-R, which bind to the substrate-binding site of the enzyme and are noncompetitive with ATP [27]. The two pyridoisoquinolines reported here exhibit a mechanism of ALK inhibition, different from that of the other known inhibitors of this enzyme and this might translate into different pharmacological properties. As far as we know, this is the first report of a tumor-active ATP noncompetitive inhibitor of ALK.

In addition to ALK(+) lymphomas, ALK may also be implicated in the pathogenesis of other solid and hematological tumors [5]. For example, constitutively activated ALK fusions, including TPM3–ALK and TPM4–ALK, have been characterized in inflammatory myofibroblastic tumors [28]. Rare cases of large-cell B-cell lymphoma have been found to have *ALK* rearrangements [29,30]. The expression of a mutated form of ALK has also been recently reported in neuroblastomas [31,32] and the expression of ALK receptor protein or fusion proteins (or both) have been described for malignant peripheral nerve sheath tumors and leiomyosarcomas [33]. Previous studies have implicated ALK signaling as a rate-limiting factor in the growth of glioblastomas, where ALK was found to be overexpressed [34]. More recently it has been shown that 3–6% of non-small-cell lung cancers carry a novel translocation in which the echinoderm microtubule-associated protein-like 4 (*EML4*) gene is fused to *ALK* [35–37]. However, although it is universally accepted that NPM–ALK plays a central role in promoting lymphomagenesis, ALK may not be the dominant mediator in these other cancers. It may act as a secondary event or a partner to exacerbate the malignant properties of already transformed cells and foster malignant progression. In that case, an inhibitor of ALK, with activity against other oncogenic proteins or kinases could be a more potent antitumor agent. Furthermore, clinicians have to face the problem of relapse, as almost invariably cancer patients develop drug resistance after treatment with kinase inhibitors, often because of the activation of alternative kinase pathways. Therefore, it seems reasonable to establish therapies that target several kinases associated with tumor growth. Indeed most of the novel small molecule kinase inhibitors used in the clinic target several kinases [38]. For example, imatinib (Gleevec) inhibits the tyrosine kinases BCR-ABL, c-KIT, and PDGFR and sorafenib (Nexavar) targets the RAF kinase, as well as VEGFR-2 and VEGFR-3, PDGFRβ, FLT-3, c-KIT, and RET kinases [38]. In this study, we showed that F91873 and/or F91874 exhibit inhibitory activity against IGF1-R, Aurora B, CHK1, and PLK1 kinases as well. Therefore, with a multikinase profile these dimeric pyridoisoquinoline ALK inhibitors might display antitumor efficacy against a larger number of ALK-related pathologies.

Conclusion

This study shows that F91873 and F91874 are multikinase inhibitors, with activity against ALK and antitumor efficacy against ALK(+) ALCL. Furthermore, these compounds, with a novel and original scaffold, are noncompetitive inhibitors for ATP and therefore exhibit a mechanism of action different from that of the other known inhibitors of ALK.

Therefore, they might display antitumor efficacy against ALK-related pathologies and possibly other malignancies.

Certainly, the remaining challenge is to optimize the design of these relatively large pyridoisoquinoline compounds to synthesize and evaluate more potent and possibly simplified analogs with toxicity and activity profiles compatible with a clinical use.

Acknowledgements

The authors thank Karine André, Jean-Christophe Blanchet, Caroline Castano, Caroline Dejean, Jérôme Fiol, Stéphane Gras, Marie-Laure Marionneau, Sandrine Pourtau, Sabine Roy, Aline Stennevin for their skilled technical assistance and Christel Ricome for her invaluable data-processing assistance. The authors are also very grateful to Frédéric Alby, Dr Jean-Marc Grégoire and Dr Frédéric Ausseil (UMS 2646 CNRS-Pierre Fabre) for carrying out the high-throughput screening with the ALK protein kinase.

References

1 Traxler P, Bold G, Buchdunger E, Caravatti G, Furet P, Manley P, *et al*. Tyrosine kinase inhibitors: from rational design to clinical trials. *Med Res Rev* 2001; **21**:499–512.
2 Blume-Jansen P, Hunter T. Oncogenic kinase signalling. *Nature* 2001; **41**:355–365.
3 Shawver LK, Slamon D, Ulrich A. Smart drugs: tyrosine kinase inhibitors in cancer therapy. *Cancer Cell* 2002; **1**:1171–1123.
4 Ma J, Xin X, Meng L, Tong L, Lin L, Geng M, *et al*. The marine-derived oligosaccharide sulfate (MdOS), a novel multiple tyrosine kinase inhibitor, combats tumor angiogenesis both in vitro and in vivo. *PloS ONE* 2008; **3**:1–11.
5 Chiarle R, Voena C, Ambrogio C, Piva R, Inghirami G. The anaplastic lymphoma kinase in the pathogenesis of cancer. *Nature Rev* 2008; **8**:11–23.
6 Stein H, Foss HD, Dürkop H, Marafioti T, Delsol G, Pulford K, *et al*. CD30(+) anaplastic large cell lymphoma: a review of its histopathologic, genetic and clinical features. *Blood* 2000; **96**:3681–3695.
7 Fisher P, Gatterer G, Danielczyk W. A Ki-1 (CD30)-positive human cell line (Karpas299) established from a high-grade non-Hodgkin's lymphoma, showing a 2;5 translocation and rearrangement of the T-cell receptor β-chain gene. *Blood* 1988; **72**:234–240.
8 Benz-Lemoine E, Brizard A, Huret JL, Babin P, Guilhot F, Couet D, *et al*. Malignant histiocytosis: a specific t(2;5)(p23;q35) translocation? Review of the literature. *Blood* 1988; **72**:1045–1047.
9 Mason DY, Bastard C, Rimokh R, Dastugue N, Huret JL, Kristoffersson U, *et al*. CD30-positive large cell lymphomas ('Ki-1 lymphoma') are associated with a chromosomal translocation involving 5q35. *Br J Haematol* 1990; **74**:161–168.
10 Morris SW, Kirstein MN, Valentine MB, Dittmer KG, Shapiro DN, Saltman DL, *et al*. Fusion of kinase gene, ALK, to a nucleolar protein gene, NPM, in non-Hodgkin's lymphoma. *Science* 1995; **267**:316–317.
11 Kutok JL, Aster JC. Molecular biology of anaplastic lymphoma kinase-positive anaplastic large cell lymphoma. *J Clin Oncol* 2002; **20**:3691–3702.
12 Morris SW, Xue L, Ma Z, Kinney MC. ALK positive CD30+ lymphomas: a distinct molecular genetic subtype of non-Hodgkin's lymphoma. *Br J Haematol* 2001; **113**:275–295.
13 Falini B. Anaplastic large cell lymphoma: pathological, molecular and clinical features. *Br J Haematol* 2001; **114**:741–760.
14 Iwahara T, Fujimoto J, Wen D, Cupples R, Bucay N, Arakawa T, *et al*. Molecular characterization of ALK, a receptor tyrosine kinase expressed specifically in the nervous system. *Oncogene* 1997; **14**:439–449.
15 Pulford K, Lamant L, Morris SW, Butler LH, Wood KM, Stroud D, *et al*. Detection of anaplastic lymphoma kinase (ALK) and nucleolar protein nucleophosmin (NPM)-ALK proteins in normal and neoplastic cells with the monoclonal antibody ALK1. *Blood* 1997; **89**:1394–1404.
16 Wan W, Albom MS, Lu L, Quail MR, Becknell NC, Weinberg LR, *et al*. Anaplastic lymphoma kinase activity is essential for the proliferation and survival of anaplastic large-cell lymphoma cells. *Blood* 2006; **107**: 1617–1623.
17 Galkin AV, Melnick JS, Kim S, Hood TL, Li N, Li L, *et al*. Identification of NVP-TAE684, a potent, selective, and efficacious inhibitor of NPM-ALK. *Proc Nat Acad Sci U S A* 2007; **104**:270–275.
18 Christensen JG, Zou HY, Arango ME, Li Q, Lee JH, McDonnell SR, *et al*. Cytoreductive antitumor activity of PF-2341066, a novel inhibitor of anaplastic lymphoma kinase and c-Met, in experimental models of anaplastic large-cell lymphoma. *Mol Cancer Ther* 2007; **6**:3314–3322.
19 Lamant L, Espinos E, Duplantier M, Dastugue N, Robert A, Allouche M, *et al*. Establishment of a novel anaplastic large-cell lymphoma-cell line (COST) from a small-cell variant of ALCL. *Leukemia* 2004; **18**:1693–1698.
20 Kruczynski A, Colpaert F, Tarayre JP, Mouillard P, Fahy J, Hill BT. Preclinical in vivo antitumor activity of vinflunine, a novel fluorinated *Vinca* alkaloid. *Cancer Chemother Pharmacol* 1998; **41**:437–447.
21 Hendricks HR, Langdon S, Dietmar PB, Breistol HH, Fodstad O, Schwartsmann G. Comparative antitumor activity of vinblastine-isoleucinate and related *Vinca* alkaloids in human tumor xenografts. *Eur J Cancer* 1992; **28A**:767–773.
22 Yamamoto O, Shirouchi Y. Benzoquinolizine derivatives and medicinal compositions. Eur. Patent. Appl. EP 0897923; 2006.
23 Dolence JM, Cassidy PB, Mathis JR, Poulter CD. Yeast protein farnesyltransferase: steady-state kinetic studies of substrate binding. *Biochemistry* 1995; **34**:16687–16694.
24 Armitage JO, Mauch PM, Harris NL, Bierman P. Non-Hodgkin's lymphoma. In: Devita VT Jr, Hellman S, Rosenberg SA, editors. *Cancer: principle and practice of oncology*. 6th ed. Philadelphia: Lippincott Williams & Wilkins; 2001. pp. 2256–2316.
25 Gumireddy K, Baker SJ, Cosenza SC, John P, Kang AD, Robell KA, *et al*. A non-ATP-competitive inhibitor of BCR-ABL overrides imatinib resistance. *Proc Natl Acad Sci U S A* 2005; **102**:1992–1997.
26 Steiner L, Blum G, Friedmann Y, Levitzki A. ATP non-competitive IGF-1 receptor kinase inhibitors as lead anti-neoplastic and anti-papilloma agents. *Eur J Pharmacol* 2007; **562**:1–11.
27 Canela N, Orzaez M, Fucho R, Mateo F, Gutierrez R, Pineda-Lucena A, *et al*. Identification of an hexapeptide that binds to a surface pocket in cyclin A and inhibits the catalytic activity of the complex cyclin-dependent kinase 2-cyclin A. *J Biol Chem* 2008; **281**:35942–35953.
28 Lawrence B, Perez-Atayde A, Hibbard MK, Rubin PB, Dal Cin P, Pinkus JL, *et al*. TPM3-ALK and TPM4-ALK oncogenes in inflammatory myofibroblastic tumors. *Am J Pathol* 2000; **157**:377–384.
29 Gascoyne RD, Lamant L, Martin-Subero JI, Lestou VS, Harris NL, Müller-Hermelink HK, *et al*. ALK-positive diffuse large B-cell lymphoma is associated with *Clathrin-ALK* rearrangements: report of 6 cases. *Blood* 2003; **102**:2568–2573.
30 Onciu M, Behm FG, Downing JR, Shurtleff SA, Raimondi SC, Ma Z, *et al*. ALK-positive plasmablastic B-cell lymphoma with expression of the *NPM-ALK* fusion transcript: report of 2 cases. *Blood* 2003; **102**:2642–2644.
31 Lamant L, Pulford K, Bishoff D, Morris SW, Mason DY, Delsol G. Expression of the ALK tyrosine kinase gene in neuroblastoma. *Am J Pathol* 2000; **156**:1711–1721.
32 Mossé YP, Laudenslager M, Longo L, Cole KA, Wood A, Attiyeh EF, *et al*. Identification of ALK as a major familial neuroblastome predisposition gene. *Nature* 2008; **455**:930–935.
33 Cessna MH, Zhou H, Sanger WG, Perkins SL, Tripp S, Pickering D. Expression of ALK1 and p80 in inflammatory myofibroblastic tumor and its mesenchymal mimics: a study of 135 cases. *Mol Pathol* 2002; **15**:931–938.
34 Lu KV, Jong KA, Kim GY, Singh J, Dia EQ, Yoshimoto K, *et al*. Differential induction of glioblastoma migration and growth by two forms of pleiotrophin. *J Biol Chem* 2005; **280**:26953–26964.
35 Soda M, Choi YL, Enomoto M, Takada S, Yamashita Y, Yishikawa S, *et al*. Identification of the transforming EML4-ALK fusion gene in non-small-cell lung cancer. *Nature* 2007; **448**:561–566.
36 Rikova K, Guo A, Zeng Q, Possemato A, Yu J, Haack H, *et al*. Global survey of phosphotyrosine signaling identifies oncogenic kinases in lung cancer. *Cell* 2007; **131**:1190–1203.
37 Inamura K, Takeuchi K, Yogashi Y, Nomura K, Ninomiya H, Okui M, *et al*. EML4-ALK fusion is linked to histological characteristics in a subset of lung cancers. *J Thorac Oncol* 2008; **3**:13–17.
38 Li R, Morris SW. Development of anaplastic lymphoma kinase (ALK) small-molecule inhibitors for cancer therapy. *Med Res Rev* 2008; **28**: 372–412.